KSCE Journal of Civil Engineering (2018) 22(12):4955-4963

DOI 10.1007/s12205-016-0765-1

Structural Engineering

pISSN 1226-7988, eISSN 1976-3808
www.springer.com/12205

A Comparative Study on Seismic Performance of Precast Shear Walls Designed with Different Variables

Wei Huang*, Min Zhang, and Zengke Yang*****

Received April 6, 2016/Revised November 16, 2017/Accepted May 4, 2018/Published Online November 8, 2018

Abstract

In order to assess the behavior of the precast shear walls with three different variables and promote the application of the new types of precast shear walls in structures, six precast shear walls with boundary elements designed based on Chinese code for design of concrete structures were tested under quasi-static cyclic loading. The three variables are reinforcement type, horizontal connection and vertical connection. In particular, there are three types of reinforcement, which are uniform, 3 × 3 and 4 × 4; three types of horizontal connection, which are dovetail joint, T-shape slot and rough surface; two types of vertical connection , which are welding and slurry sitting. Tests results indicate that the failure mode of specimens SW-1 through SW-5 was diagonal tension failure and failure mode of specimen SW-6 was shear sliding; the three variables have effect on peak load, drift ratios and ductility; the combination of reinforcement type "4 × 4", dovetail joint and welding make an improvement on peak load, ductility and energy dissipation; while the T-shape slot is not applicative preferentially in horizontal connection and the slurry sitting vertical connection type is not recommended in mid-rise buildings.

Keywords: *seismic performance, precast shear wall, horizontal connection, vertical connection, reinforcement type*

1. Introduction

With advantages of fast construction, energy-saving, environmental protection and low cost, precast shear wall structure is suitable for residential construction industry architecture. At present in China, with the rapid development of construction industry and housing industrialization, construction technology of precast shear wall structure is becoming an urgent matter.

In recent years, studies on the structural performance of components and nodes connections in precast shear structural system have been carried out. Some scholars (Kurama *et al.*, 2006; Kurama *et al.*, 2008)investigated the performance of the unbonded post-tensioned hybrid coupled wall structures, and test results showed that it was feasible to use unbonded posted-tensioned technology in connections between walls. Meanwhile, the seismic behavior of precast reinforced concrete shear walls using different ways vertical reinforcement connection were invonestigated to assess the new vertical connection (Qian *et al.*, 2011; Qian *et al.*, 2011). Test results indicated that the stresses of vertical reinforcements can be transferred effectively by grout sleeves and the failure mode of the precast concrete shear wall specimens is the same as that of the cast-in-site wall specimen, i.e., tensile yield of reinforcements and compressive failure of concrete. An improved on grout sleeve splicing was made and studied the seismic behaviors of precast shear walls with vertical distributed reinforcements spliced by a single row of steel bars indirect splicing (Zhang *et al.*, 2012). The test results indicated that the vertical rebars yield before the specimens reach their ultimate strengths, the concrete crushes at the bottom of the wall, and the failure mode of all specimens is compression-bending. In order to promote building and housing industrialization, tests on joints of new precast concrete shear wall structure were carried out (Zhu *et al.*, 2012), and test results showed that precast specimens have similar seismic behaviors with the cast-in-situ specimens. Some scholars investigated the carrying capacity, deformation behavior, and the property of energy absorption of the superimposed slab shear walls (Ye *et al.*, 2009), found that it is possible to replace the RC shear wall with the superimposed slab shear wall under the necessary conditions, and they gave a suggestion that it is recommended to set shear reinforcement or shear oblique groove at wall base. Although a large amount of experimental researches have been conducted, additional studies should be performed to promote the knowledge and application of these kinds of connections in precast shear wall structures, especially experiments on large-scale precast reinforced concrete shear wall structure. Previously, a three-story full-scale model for

*Professor, College of Civil Engineering, Xi'an University of Architecture and Technology, Xi'an 710055, China (E-mail: qqhuangwei2005@126.com)
**Lecturer, School of Management Science and Engineering, Hebei University of Economics and Business, Shijiazhuang 050061, China (Corresponding Author, E-mail: mzhangsjz528@163.com)
***Lecturer, College of Civil Engineering, Henan Polytechnic University, Jiaozuo 454000, China (E-mail: 94027203@qq.com)

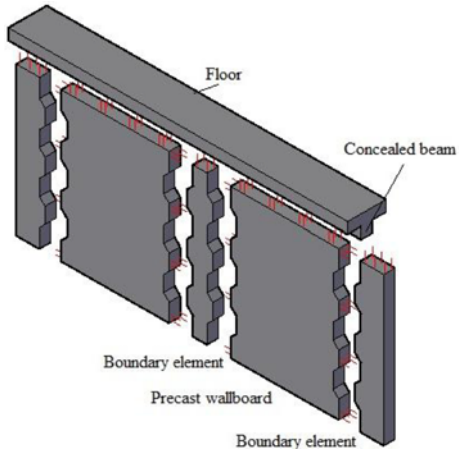

Fig. 1. Construction Details of Precast Shear Wall

an elastic quasi-static was tested (Jiang *et al.*, 2011). Test results indicated that the overall seismic energy dissipation capacity of the structure can be enhanced if the connections between precast members have adequate deformation capacities, and further experimental and theoretical studies need to be carried out so that it can be applied in seismic design of practical engineering.

In order to solve these problems which are technically challenging and cost prohibitive in existing connections ways (Zhang *et al*., 2012; Zhu *et al*., 2012; Jiang *et al*., 2011; Zhang *et al*., 2014), a new precast concrete wall structure is proposed based on the previous research, i.e. the ecological composite wall structure (Chen *et al*., 2012; Liu *et al*., 2010; Liu *et al*., 2013). The precast concrete wall structure is composed of precast wallboard, cast-in-situ boundary elements, and the floor, as shown in Fig. 1.

In this study, six 1/2-scale precast shear wall specimens were designed and tested under quasi-static cyclic loading to evaluate the seismic behavior of the new precast wall and giving design suggestions. In this study, effect of three parameters on the crack patterns and failure modes, peak load, drift capacity, stiffness degradation, and energy dissipation are compared and analyzed, respectively. The experimental results of six specimens can be used as reference for engineering practice of precast shear wall structure.

2. Experimental Program

2.1 Test Specimens

Six specimens with a height to length ratio of 0.96 were tested to provide information on shear strength and drift capacity of precast shear wall, and to evaluate shear requirements specified by Chinese code for design of concrete structures GB50010-2010 (2010) and Technical specification for precast composite wall structure DBJ61/T 94-2015 (2015). And the objectives that the tested walls must reach to have a good performance, in particular the elastic displacement angle and elastoplastic interlayer displacement angle are 0.1% and 8.3%. The testing program consisted of three variables, which are reinforcement type, horizontal connection type and vertical connection type, such that a direct comparison could be made, as shown in Table 1.

Table 1. Characteristics of Specimens

No.	Reinforcement type	Horizontal connection type	Vertical connection type
SW-1	Uniform	Dovetail joint	Welding
SW-2	3 × 3	Dovetail joint	Welding
SW-3	4 × 4	Dovetail joint	Welding
SW-4	4 × 4	T-shape slot	Welding
SW-5	4 × 4	Rough surface	Welding
SW-6	4 × 4	Dovetail joint	Slurry sitting

The precast wallboard has a length of 950 mm, a height of 1350 mm and a thickness of 100 mm. With a 200 mm length cast-in-situ boundary element and a 25 mm length construction joint each side, all specimens have a overall length of 1400 mm. The height from the top surface of foundation beam to the action

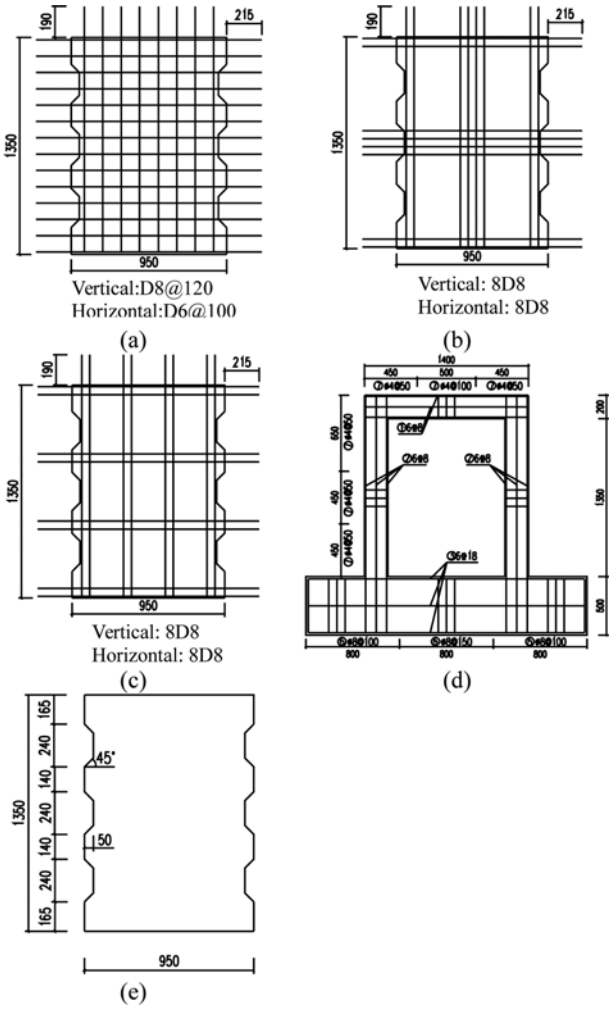

Fig. 2. Geometry and Reinforcement Layout of Specimens: (a) Precast Wallboard of Uniform Reinforcement, (b) Precast Wallboard of 3 × 3 Reinforcement, (c) Precast Wallboard of 4 × 4 Reinforcement, (d) Shell Frame, (e) Geometry of Shear Keys

point of lateral loading is 1450 mm. The geometry and reinforcement layout of specimens are illustrated in Fig. 2.

The precast wallboard of all specimens were vertically web reinforced with eight hot rolled ribbed bars D8 (diameter = 8 mm), constituting a vertically web reinforcement ratio ρ_v of 0.85%. Hot rolled ribbed bars D6 (diameter = 6 mm) spaced at 100 mm (D6@100) were used as the horizontal web reinforcement of specimen SW-1 (shown as Fig. 2(a)), and eight hot rolled ribbed bars D8 (diameter = 8 mm) were used as the horizontal web reinforcement of specimen SW-2 (shown as Fig. 2(b)), and specimens SW-3 through SW-6 (shown as Fig. 2(c)), constituting a horizontal web reinforcement ratio ρ_h of 0.60%. Six hot rolled ribbed bars D8 (diameter = 8 mm) were used as the vertical reinforcement of the boundary of all specimens, constituting a longitudinal reinforcement ratio ρ of 1.51%; and transversely reinforced with hot rolled plain bars D4 (diameter = 4 mm) hoops and ties spaced at 50 mm (D4@50).

Three kinds of horizontal connection were used in this study, as shown in Fig. 3. Dovetail joint was used as the horizontal connection between wallboard and boundary element of specimens SW-1 through SW-3, and specimen SW-6 (shown as Fig. 3(a)); T-shape slot was used as the horizontal connection between wallboard and boundary element of specimen SW-4 (shown as Fig. 3(b)); and Rough surface was used as the horizontal connection between wallboard and boundary element of specimen SW-5 (shown as Fig. 3(c)).

Two kinds of vertical connection types were used in this study, as shown in Fig. 4. Welding was used as vertical connection between wallboard base and foundation beam of specimens SW-1 through SW-5 (shown as Fig. 4(a)); Slurry sitting was used as vertical connection between wallboard base and foundation beam of specimen SW-6 (shown as Fig. 4(c)). The construction details of welding are shown in Fig. 4(b). There were plates with two hot rolled ribbed bars D14 bended like U wielded on each as dowel reinforcement. Two plates are embedded in wallboard and other two plates embedded in foundation beam. The length of the dowel bars extended into the wallboard and into the foundation was 300 mm.

The construction of specimens mainly includes the following three steps: (1) construction of foundation beam; (2) prefabrication of wallboard; (3) assembly of the wallboard and the cast-in-situ boundary elements. The construction procedures are shown in Fig. 5.

2.2 Mechanical Properties oF Material

In this study, the mix proportion of concrete: cement: sand: aggregate = 1: 2.3: 4.2; water/cement = 0.49. The cement is P.O32.5 ordinary Portland cement, the fine aggregate is medium sand, and the size of aggregate is 5-20 mm. Several cubes of 150 mm side length were prepared and cured in the laboratory in a water bath under a temperature of 20°±2°C and then tested at the age of 28 days for compressive strength and tensile splitting

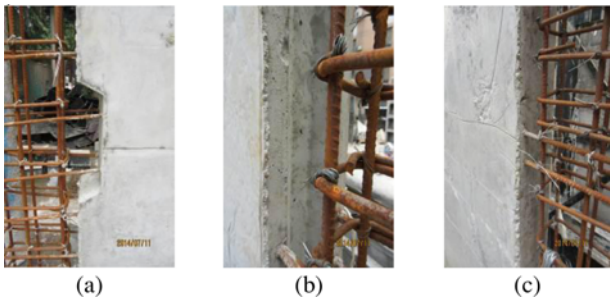

Fig. 3. Horizontal Connection Types: (a) Dovetail Joint, (b) T-shape Slot, (c) Rough Surface

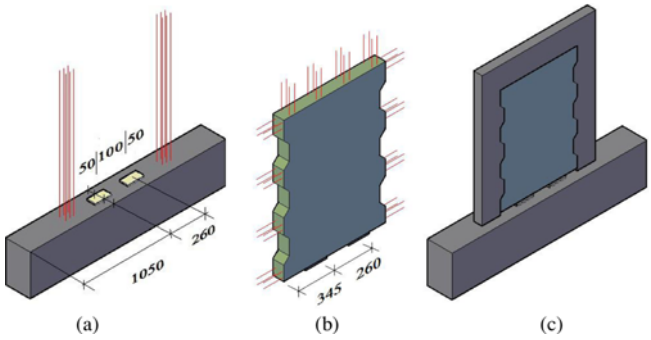

Fig. 5. Vertical Connection Types: (a) Construction of Foundation Beam, (b) Prefabrication of Wallboard, (c) Assembly of Wallboart and Boundary Elements

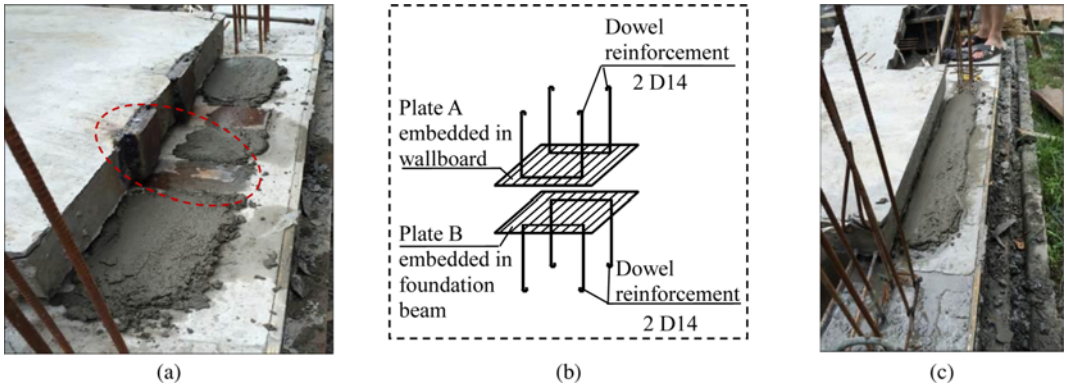

Fig. 4. Vertical Connection Types: (a) Welding, (b) Details of Welding, (c) Slurry Sitting

Table 2. Mechanical Properties of Reinforcement

Type	Yield strength f_y / MPa	Ultimate strength f_u / MPa	Elastic modulus E_s / MPa
D4	368	467	2.1×10^5
D6	456	569	2.0×10^5
D8	445	555	2.0×10^5
D14	467	618	2.0×10^5

strength. The average of three values was recorded as the strengths of concrete. The average cube crushing strength of concrete is 29.5 MPa, and average tensile splitting strength is 18.6 MPa. Several standard prisms of 150 mm × 150 mm × 300 mm were prepared and cured in the laboratory in a water bath under a temperature of 20° ± 2°C and then tested at the age of 28 days for axial compressive strength and elastic modulus. The average of three values was recorded as the strengths of concrete. The average compressive strength of concrete is 25.1 MPa, and the elastic modulus is 29.8 GPa. The mechanical properties of reinforcement are shown in Table 2.

2.3 Test Setup

The horizontal load was applied on the specimens by a double-acting actuator with a capacity of ±1,000 kN, as shown in Fig. 6(a). While the axial load was applied with a hydraulic jack on the steel beam which was placed on the top of the RC coupling beam to simulate the vertical pressure of the underlying wall in the actual project. The value of the axial load is 700 kN, calculated according to the axial compression ratio of the ground wall of a 12 layer precast shear wall structure. The steel beam was used for making sure that the axial load could be applied uniformly to the specimens. Fig. 6 shows a front view and a side view of the test setup.

2.4 Instrumentation

A series of LVDTs, i.e., liner variable displacement transducers, were applied to measure the deformations of specimens. One 200 mm LVDT was used to measure the top displacement at the application point of lateral load, and the other one LVDT was

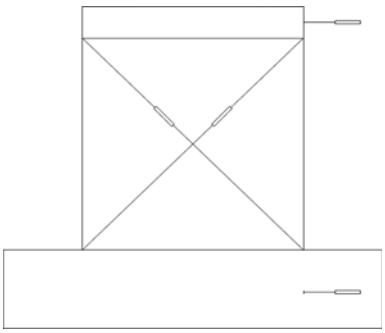

Fig. 7. Instrumentation of Specimens

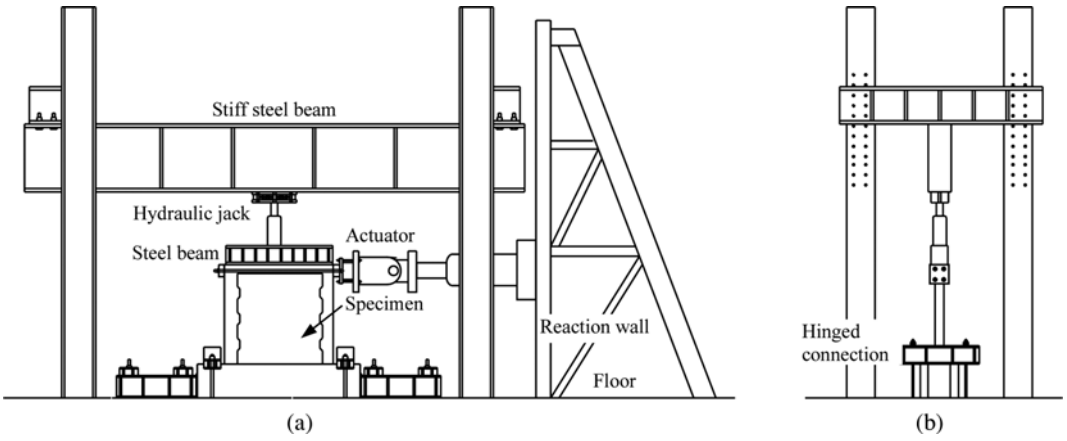

Fig. 6. Test Setup: (a) Front View, (b) Side View

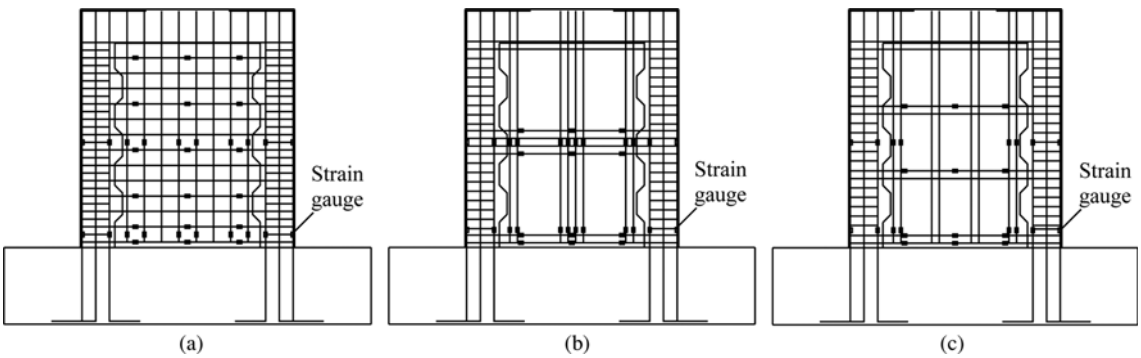

Fig. 8. Measured Stain Gauges: (a) SW-1, (b) SW-2, (c) SW-3, SW-4, SW-5 and SW-6

installed at the foundation beam to measure the sliding displacement of the specimens. Moreover, to measure the bending deformation and shear deformation of the specimens, two more LVDTs were installed in the diagonal directions, as shown in Fig. 7.

The electrical resistance strain gauges were mounted on some selected vertical and horizontal reinforcements to monitor and analysis the steel strain during the test. Fig. 8(a) and Fig. 8(b) show the selected locations of stain gauges in specimen SW-1 and SW-2, respectively. While, the selected locations of stain gauges in specimens SW-4 through SW-6 were same as specimen SW-3, as shown in Fig. 8(c).

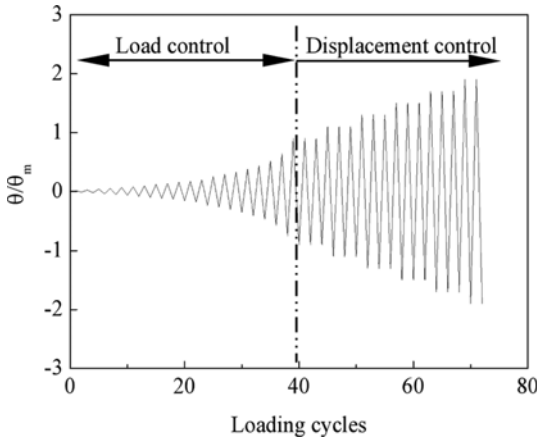

Fig. 9. Loading Procedure

2.5 Loading Procedure

The observed loading procedure during tests is shown in Fig. 9; θ_m indicates the rotational angle corresponding to the displacement of the coupling beam when the specimen reaches the ultimate load. The axial load were invariant when the cyclic lateral load was applied to the specimens. At the first state, force control was taken with an increasing amplitude of 30 kN, and for each load level one cycle was applied. After that, displacement control was conducted. The ductility level was 2 mm per amplitude, and for each ductility level three cycles were applied.

3. Test Results

3.1 Crack Patterns and Failure Modes

According to the test, the failure process of most walls can be classified into three stages, namely elastic stage, elastic-plastic stage and failure stage, while the pictures taken at the failure stage of six walls are shown in Fig. 10, respectively. But due to the difference of the design variables, the failure mechanisms of the specimens are different.

For evaluating the observed behaviors of the specimens, three failure modes were identified (Julian *et al*., 2015). The first mode is diagonal tension failure. This is related to concrete inclined cracking, no web crushing of concrete, and yielding or plastic yielding of most longitudinal reinforcement of boundary element. The second mode was diagonal compression failure and is related to yielding of some steel bars or wires and noticeable web

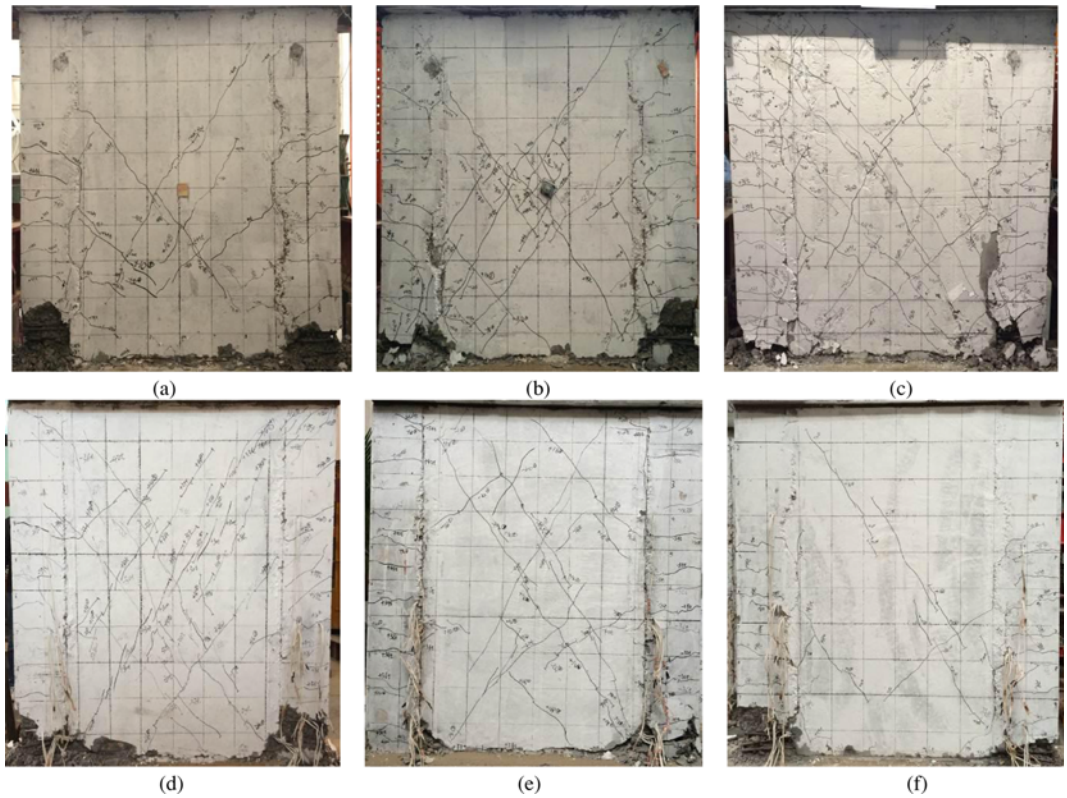

Fig. 10. Crack Patterns of Specimens at Failure Load: (a) SW-1, (b) SW-2, (c) SW-3, (d) SW-4, (e) SE-5, (f) SW-6

crushing and spalling of concrete. A compression failure may occur without significant plastification of web steel. This is particularly the case when low strength concrete and/or large steel ratios are used. The third mode is sliding shear failure, which is characterized by resisting shear force by aggregate interlock of concrete in the compression zone and dowel action of the vertical connections.

The final crack patterns of all specimens are shown in Fig. 10. Failure mode of specimens SW-1 through SW-5 was diagonal tension failure whereas diagonal compression failure mode was not observed in specimens. Besides, failure mode of specimen SW-6 was shear sliding at the vertical connection of slurry sitting after diagonal tension was observed at the wallboard.

3.2 Hysteresis Curves

Figure 11 shows the hysteresis curves of all specimens obtained the test, from which we can see that the hysteresis loops of all specimens were typical of concrete walls controlled by shear deformations. And although pinching of hysteresis loops was observed, the loops of all specimens were nearly stable and symmetric during tests.

Based on the above introduced hysteresis curves, some useful performance indexes are introduced. δ in Fig. 11 is the relative displacement between the top and bottom of the specimens. Drift at cracking, ID_{cr}, is the ratio between the cracking displacement, δ_{cr}, and the height of wall, H, which is expressed as $ID_{cr} = \delta_{cr}/H$. Similarly, ID_y, ID_{max} and ID_u are associated to displacement corresponds to yielding force, δ_y, displacement corresponds to peak force, δ_p, and ultimate displacement, δ_u. Ductility, μ, is the ratio between the ultimate displacement, δ_u, and the yielding force, δ_y. The parameters measured during tests of specimens are summarized in Table 3.

To evaluate the deformation capability of the specimen, a ratio of the horizontal displacement at the top of the specimen to the height of the specimen is defined, which is represented as $ID = \delta/H$. It's used to limit the horizontal displacement of structure under the normal use condition, to ensure the high-level structure's stiffness, and to avoid producing too large displacement and influence the bearing capacity, stability and use requirements of structure.

In general, specimen SW-3 exhibited a larger forces (increase by 4% ~ 6% at peak state), and the strong crushing at the corners of specimens SW-1 and SW-2 effect reduces the capacity of the concrete in compression, leading to decrease the drift ratios and

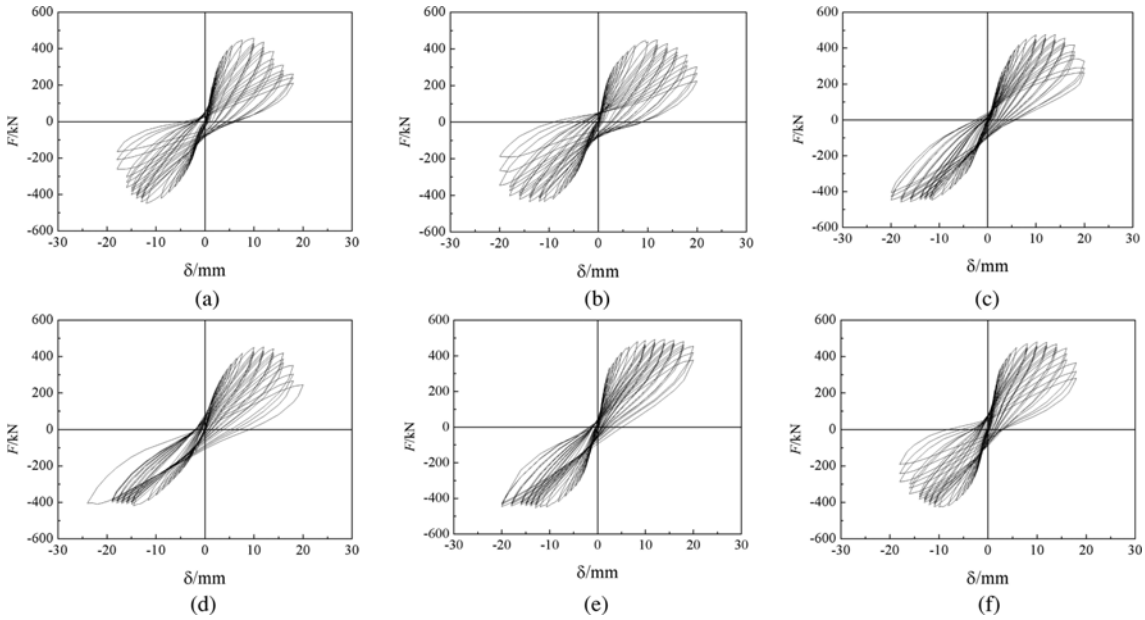

Fig. 11. Hysteresis Curves of Specimens: (a) SW-1, (b) SW-2, (c) SW-3, (d) SW-4, (e) SW-5, (f) SW-6

Table 3. Main Parameters of Response Measured on Specimens

No.	Force				Drift ratio				μ
	F_{cr} (kN)	F_y (kN)	F_p (kN)	F_u (kN)	ID_{cr} (%)	ID_y (%)	ID_p (%)	ID_u (%)	
SW-1	299.07	359.33	457.30	385.22	0.18	0.25	0.67	0.87	3.50
SW-2	241.99	361.74	449.65	367.81	0.14	0.33	0.87	1.19	3.60
SW-3	268.36	359.50	476.34	417.60	0.20	0.32	0.93	1.19	3.76
SW-4	272.72	361.12	453.43	386.98	0.21	0.36	0.80	1.06	3.52
SW-5	247.84	390.30	491.95	418.37	0.13	0.27	0.93	1.33	4.86
SW-6	299.35	389.81	481.50	415.08	0.14	0.21	0.67	1.06	4.20

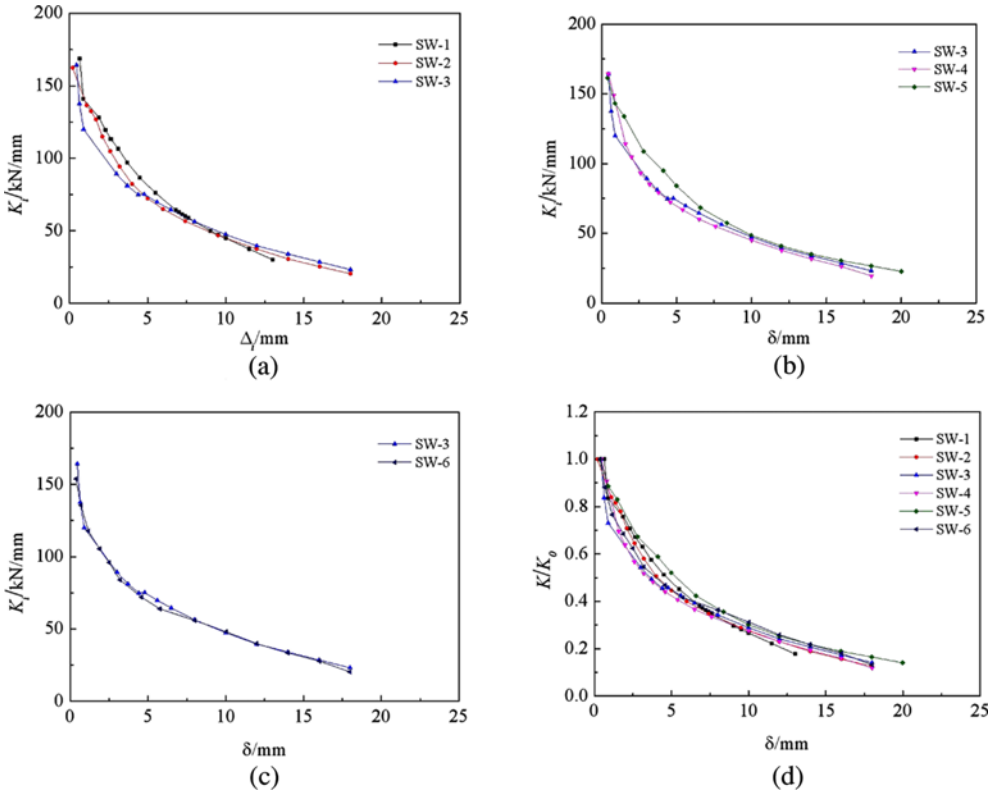

Fig. 12. Stiffness Degradadion: (a) Reinforcement Type, (b) Horizontal Connection Type, (c) Vertical Connection Type, (d) Relative Stiffness

ductility, which means the "4 × 4" reinforcement type has a better performance than the other two reinforcement types. Whereas compared with specimen SW-4, specimens SW-3 and SW-5 exhibited larger force values, drift ratios and ductility, which shows that horizontal connection types of dovetail joint and rough surface, other than the T-shape slot, made the wallboard and boundary elements work as one unit. Although specimen SW-6 got a similar peak force value and ductility with specimen SW-3, lower drift ratios because of the sliding of the slurry sitting vertical connection type are observed. And the slurry sitting vertical connection type is not recommended in high-rise buildings.

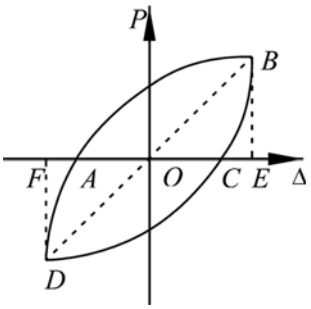

Fig. 13. Calculation of Energy Dissipation Coefficient

3.3 Initial Stiffness and Stiffness Degradation

In order to evaluate the influence of the three key parameters on wall stiffness, the initial stiffness and stiffness degradation were calculated and plotted in Figs. 6(a), (b) and (c), respectively. It is evident that initial stiffness value of specimen SW-6 is smaller than the values of other five specimens, which are nearly the same. The relation between displacement δ and relative stiffness K/K_0 of all specimens are plotted in Fig. 6(d), from which we can see that specimen SW-5 shows a lower value of stiffness degradation than the other specimens, especially specimen SW-4, which indicates that the T-shape slot is not applicative preferentially in horizontal connection.

3.4 Energy Dissipation

In a cyclic loading process, the energy dissipation due to inelastic deformation is generally represented with the area surrounded by the load-deformation hysteresis curve. And to evaluate the energy dissipation capacity of the precast shear wall specimen, a coefficient E, i.e. the energy dissipation coefficient (Dang *et al.*, 2014) is defined and cited, which is calculated as follows:

$$E = \frac{S_{A\widehat{B}C+C\widehat{D}A}}{S_{\Delta OBE}+S_{\Delta ODF}} \tag{1}$$

Where $S_{A\widehat{B}C+C\widehat{D}A}$ is the area within hysteresis loop, i.e. the energy dissipated by the specimen in a single hysteresis cycle; $S_{\Delta OBE}$ and $S_{\Delta ODF}$ represent the area of triangle OBE and the area of triangle ODF, respectively.

Figure 13 shows the calculation parameters in Eq. (1).

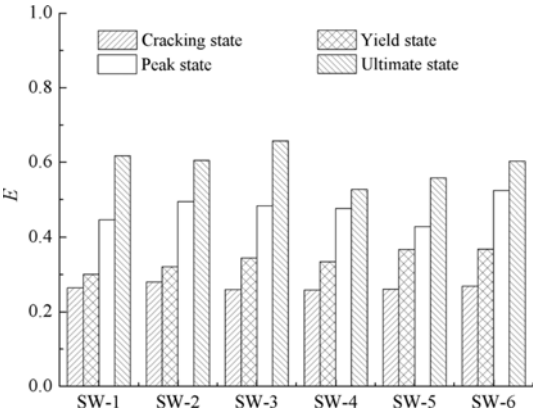

Fig. 14. Energy Dissipation Coefficient *E* of Specimens

Energy dissipation coefficient *E* of all specimens at four states are calculated by using Eq. (1), as shown in Fig. 14.

From the above figure, some conclusions can be obtained that all specimens reaches yield state energy accounted for 45% ~ 59% of energy dissipation at peak state, the average is 52%; and all specimens reaches peak state accounted for 68% ~ 91% of energy dissipation at ultimate state, the average is 79%. From cracking state to ultimate state, the energy dissipation coefficient *E* shows a steady upward trend, which indicates the cumulative energy dissipation. It's evident that *E* of specimen SW-3 are larger than the other specimens, which show that the combination of reinforcement type "4 × 4", vertical connection type "dovetail joint" and horizontal connection type "welding" is more conducive to the dissipation of energy.

4. Conclusions

An experimental study that comprised quasi-static cyclic tests of six precast shear walls was conducted to provide information on seismic performance of walls in terms of crack patterns, failure modes, hysteresis curves, initial stiffness, stiffness degradation and energy dissipation. The main results obtained from the tests can be summarized as follows.

1. The failure mechanism is different due to the design variables. Failure mode of specimens SW-1 through SW-5 was diagonal tension failure and failure mode of specimen SW-6 was shear sliding at the vertical connection of slurry sitting after diagonal tension was observed at the wallboard.
2. The three key parameters, i.e. reinforcement type, horizontal connection type and vertical connection type, all have effect on peak load, drift ratios and ductility, when the web reinforcements remains constant. The combination of reinforcement type "4 × 4", vertical connection type "dovetail joint" and horizontal connection type "welding" make an improvement of peak load, ductility and energy dissipation but small decrease in initial stiffness than the other specimens SW-1 and SW-2; while SW-5 has a slightly higher peak force and a significant performance in ductility than SW-3.
3. The T-shape slot is not applicative preferentially in horizontal connection, and the slurry sitting vertical connection type is not recommended in mid-rise buildings. However, the practical application of the precast shear wall should be further compared and investigated.

Acknowledgements

The authors gratefully acknowledge the financial support provided by the National Natural Science Foundation of China (51378416 and 51578446).

References

Chen, G. X., Huang, W., and Zhang, Y. (2012). "Study on a seismic performance of a multi-ribbed composite wall filled in different materials block." *Journal of Central South University*, Vol. 43, No. 11, pp. 4991-4500.

Dang, Z., Liang, X. W., Deng, M. K., Li, F. Y., and Yu, J. (2014). "Experimental and theoretical studies on seismic behavior of fiber reinforced concrete shear walls." *Journal of Building Structures*, Vol. 35, No. 6, pp. 12-22, DOI: 10.14006/j.jzjgxb.2014.06.003.

DBJ61/T 94-2015 (2015). *Technical specification for precast composite wall structure,* Shanxi Council, China Building Material Press, Beijing, China.

GB50010-2010 (2010). *Code for design of concrete structures*, Ministry of Housing and Urban-Rural Development of the People's Republic of China, China Architecture & Building Press, Beijing, China.

Jiang, H. B., Chen, Z. X., Zhang J. Q., Wu, B., Tian, Y. B., and Liu, W. Q. (2011). "Quasi-static test of precast reinforced concrete shear wall structure." *Journal of Building Structures*, Vol. 32, No. 6, pp. 34-40, DOI: 10.14006/j.jzjgxb.2011. 06.011.

Julian, C., Juan, M. L., and Ricardo, B. (2015). "Effect of lightweight and low-strength concrete on seismic performance of thin lightly-reinforced shear walls." *Engineering Structures*, Vol. 93, pp. 61-69, DOI: 10.1016/j.engstruct.2015.03.022.

Kurama, Y. C. and Shen, Q. (2008). "Seismic design and response evaluation of unbonded post-tensioned hybrid coupled wall structures." *Earthquake & Structural Dynamics*, Vol. 37, No. 14, pp. 1677-1702, DOI: 10.1002/eqe.852.

Kurama, Y. C., Weldon, B. D., and Shen, Q. (2006). "Experimental evaluation of post-tensioned hybrid coupled wall subassemblages." *Journal of Structural Engineering-asce*, Vol. 132, No. 7, pp. 1017-1029, DOI: 10.1061/(ASCE)0733-9445(2006)132:7(1017).

Liu, P. and Siu-Kui, A. (2013). "Bayesian parameter identification of hysteretic behavior of composite walls." *Probabilistic Engineering Mechanics*, Vol. 34, pp. 101-109, DOI: 10.1016/j.probengmech. 2013.08.005.

Liu, P. and Yao, Q. F. (2010). "Dynamic reliability of structures: The example of multi-grid composite walls." *Structural Engineering and Mechanics*, Vol. 36, No. 4, pp. 463-479, DOI: 10.12989/sem.2010. 36.4.463.

Qian, J. R., Peng, Y. Y., Zhang, J. M., Qin, H., Li, J. S., Liu, G. Q., Zhao, F. D., and Li, L. R. (2011). "Tests on seismic behavior of pre-cast shear walls with vertical reinforcements spliced by grout sleeves." *Building Structures*, Vol. 41, No. 2, pp. 1-6.

Qian, J. R., Yang, X. K., Qin, H., Peng, Y. Y., Zhang, J. M., and Li, J. S. (2011). "Tests on seismic behavior of pre-cast shear walls with various methods of vertical reinforcement splicing." *Journal of*

building Structures, Vol. 32, No. 6, pp. 51-59, DOI: 10.14006/j.jzjgxb.2011.06.013.

Ye, X. G., Zhang, L. J., Wang, D. C. i., and Jiang, Q. (2009). "Experimental study on horizontal carrying capacity of superimposed slab shear walls." *Journal of Hefei University of Technology*, Vol. 32, No. 8, pp. 1215-1218.

Zhang, X. Z., Han, P., Li, Y. L., Wang, J. C., and Ling, G. R. (2014). "Seismic behavior of prefabricated alveolar type RC shear walls with cast-in-place embedded columns." *Journal of Building Structures*, Vol. 35, No. 8, pp. 88-94.

Zhang, W. J., Qian, J. R., Yu, J. S., Qin, H., and Liu, G. Q. (2012). "Tests on seismic behavior of precast share walls with boundary elements and vertical distributed reinforcements spliced by a single row of steel bars." *China Civil Engineering Journal*, Vol. 45, No. 10, pp. 89-97, DOI: 10.15951/j.tmgcxb.2012.10.015.

Zhu, Z. F. and Guo, Z. X. (2012). "Seismic test and analysis of joints of new precast concrete shear wall structures." *China Civil Engineering Journal*, Vol. 45, No. 1, pp. 69-76, DOI: 10.15951/j.tmgcxb.2012.01.020.